

# Silicon-on-Insulator Single Electron Transistors

F. O. Heinz<sup>a</sup>, A. Schenk and W. Fichtner

**Keywords:** Single Electron Devices, 3D, Coulomb Blockade, Quantisation, Device Simulation

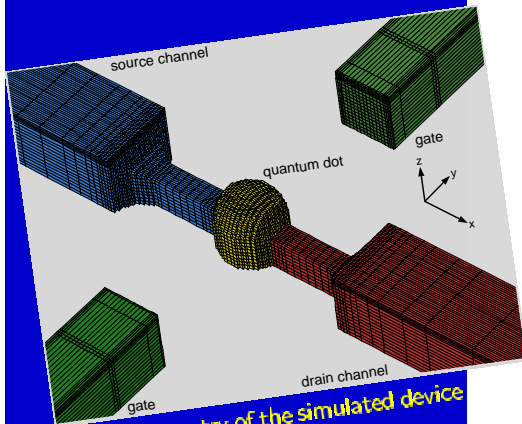


Fig. 1: Geometry of the simulated device (derived from [1])

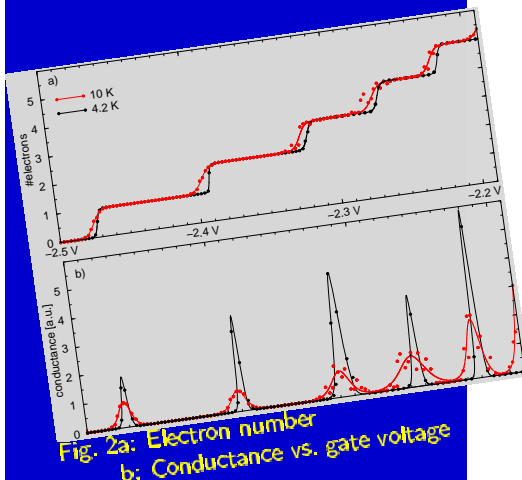


Fig. 2a: Electron number  
b: Conductance vs. gate voltage

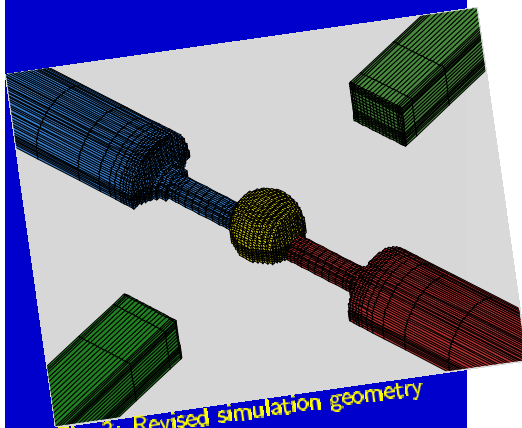


Fig. 3: Revised simulation geometry

Single Electron Transistors (SET) are voltage controlled switching devices which might be suitable for miniaturisation beyond the limit for traditional field effect transistors (FET).

An SET consists mainly of an *island*, that weakly couples to *source* and *drain* leads via tunneling contacts (the constrictions in fig. 1), and a *gate* (in our case a pair of gates) for capacitive tuning of the island. The operation of an SET is based on *Coulomb blockade*, i.e. the fact that charge can tunnel on and off the island only in units of the elementary charge  $e$ , which results in the blocking of conduction if the

electrons lack the energy necessary for charging the island. For large islands this energy is defined by the island capacitance, thereby giving rise to the “orthodox theory” (cf. e.g.[2]) of SETs with its periodic  $I$ - $V$  characteristic.

In very small islands (“quantum dots”) the discreteness of the allowed electron energies needs to be taken into account.

In terms of the single particle eigenstates  $\epsilon_p^N$  of the quantum dot with total occupancy  $N$  the linear response conductance of the quantised SET may then be written according to Beenakker [3] as

$$G = \frac{e^2}{kT} \sum_p \sum_N \frac{\Gamma_p^l \Gamma_p^r}{\Gamma_p^l + \Gamma_p^r} P_{\text{eq}}(N) (1 - P_{\text{eq}}(n_p = 1|N)) f(\beta(\epsilon_p^N + U(N+1) + U(N) - \epsilon_F)),$$

where the  $\Gamma_p^{l/r}$  are the source/drain side tunneling rates associated with the  $\epsilon_p^N$ , and the argument to the Fermi function corresponds to the energy necessary to populate the  $p^{\text{th}}$  single particle state by increasing the total electron number from  $N$  to  $N+1$ . The  $\epsilon_p^N$  are obtained by self-consistently solving the Schrödinger–Poisson equation inside the quantum dot at various values  $\mu_i$  of a parametric quantum dot chemical potential — at this stage the individual states are assumed to be populated according to a Fermi–Dirac distribution. States with integral total  $N$  are constructed by interpolation between the  $\mu_i$ . For all  $N$  values with significant population we then compute the canonical partition function  $Z(N)$  by means of Monte Carlo sampling. This yields the conditional probabilities  $P_{\text{eq}}(n_i = 1|N)$  for the occupation of the  $i^{\text{th}}$  (non-degenerate) single-particle state at total electron number  $N$ . With the true chemical potential of the quantum dot being equal to the outside Fermi energy, we may also compute the grand canonical partition function  $\Xi$ , and consequently arrive at the equilibrium probabilities  $P_{\text{eq}}(N)$  for the various  $N$ . In conjunction with tunneling rates from Bardeen’s transfer hamiltonian method we now have all the ingredients for the computation of  $G$ .

Fig. 2a depicts the equilibrium electron number inside the quantum dot as function of the control gate voltage at two different temperatures, 4 K and 10 K; fig. 2b shows the associated linear–response conductance. Note the non–equidistant spacing of the conductance peaks. At 4 K the conductance peaks are well separated; at 10 K the peaks are much wider and are beginning to merge. At still higher temperatures thermal broadening will eliminate the conductance oscillations, altogether.

The tunneling rates  $\Gamma_p^{l/r}$  have not been taken into

account for graph 2b: In the course of running our simulations it turned out that the tunneling barriers in our simulation geometry are too weak. With more than two electrons inside the quantum dot, localisation of the wavefunctions is gradually lost due to electron–electron repulsion, and the dominant conductance mechanism changes from single electron tunneling to coherent 1D transport. But since we are concerned with tunneling transport, the tunneling rates were artificially set constant in order to push the device back into the Coulomb blockade regime. We are currently working on a revised simulation model with sufficiently strong barriers. The geometry shown in fig. 3 can accommodate some eight electrons before delocalised states become available for occupation; when seen from above it should still be in accordance with the SEM micrograph shown in [1]. With further minor alterations of the shape of the constrictions it should be possible to accommodate the 12 electrons necessary to reproduce the 12 conductance peaks observed by Kern *et al.* [1]. Then it will be meaningful to re–enable the computation of the tunneling rates, such that quantitative conductance data may be obtained.

This work was done inside the NANOTCAD project (IST–1999–10828).

- [1] Kern *et al.*; ‘Doped Silicon Single Electron Transistors with Single Island Characteristics’, *Appl. Phys. Lett.*, vol. 76, pp. 2065–2067, 2000
- [2] Likharev, K.; ‘Single-Electron Devices and Their Application’, *Proc. of the IEEE*, vol. 87, pp. 606–630, 1999
- [3] Beenakker, C. W. J.; ‘Theory of Coulomb–Blockade Oscillations in the Conductance of a Quantum Dot’, *Phys. Rev. B*, vol. 44, pp. 1646–1656, 1991

<sup>a</sup>corresponding author — address: Institut für Integrierte Systeme, Gloriastrasse 35, ETH Zürich, CH–8092 Zürich, Switzerland; phone: +41 1 632 59 57; e–mail: frederik.heinz@iis.ee.ethz.ch